Identification of tsunami deposits using a combination of radiometric dating and oxygen-isotope profiles of articulated bivalves

A. Kitamura[a, b], M. Ito[a], S. Sakai[c], Y. Yokoyama[d], Y. Miyairi[d]

[a]*Faculty of Science, Shizuoka University, 836 Oya Suruga-ku, Shizuoka 422-8529, Japan*

[b]*Center for Integrated Research and Education of Natural hazards, Shizuoka University, 836 Oya, Suruga-ku, Shizuoka 422-8529, Japan*

[c]*Institute of Biogeochemistry, Japan Agency for Marine-Earth Science and Technology, Yokosuka, Kanagawa 237-0061, Japan*

[d]*Atmosphere and Ocean Research Institute, University of Tokyo, 5-1-5 Kashiwanoha, Kashiwa, Chiba 277-8564, Japan*

ABSTRACT

Four tsunami deposits (deposits I–IV) have been identified on Ishigaki Island, southwest Japan. The youngest tsunami deposit (deposit I) was caused by the Meiwa tsunami, which occurred on 24 April AD 1771, as described in reliable historical documents. Two well-preserved specimens of articulated marine bivalve were collected from the youngest tsunami deposit (deposit I) and an additional two from the second-youngest tsunami deposit (deposit II; 920–620 cal. yr BP). The shells were tightly closed and empty inside. No encrusting epifauna or evidence of erosion was observed on the inner or outer shell surfaces. In each tsunami deposit, the ^{14}C ages of the shells are nearly identical. The mode of occurrence and coincidence of ages mean that these shells were transported and buried alive by tsunamis. We analyzed the oxygen-isotope ($\delta^{18}O$) profiles of these bivalves to determine the seasons of their death, which provides clues to the seasonal timing of tsunamis. Tsunami deposits I and

II were formed during spring and fall, respectively. The former supports the proposal that tsunami deposit I was caused by the 1771 Meiwa tsunami and provides regional radiocarbon reservoir age for the late 1700s; the latter provides a chronological constraint on the identification of tsunami deposit II. Thus, a combination of radiometric dating and $\delta^{18}O$ profiles of articulated bivalves derived from tsunami deposits provides important chronologic constraints for examining paleo-tsunami events.

Keywords: tsunami deposits; oxygen isotope profiles; articulated bivalves; Ryukyu Trench

1. Introduction

Over the last two decades, the 2004 Indian Ocean earthquake (Mw 9.1) and the 2011 off the Pacific coast of Tohoku earthquake (Mw 9.0) caused mega-tsunamis that resulted in approximately 220,000 and 20,000 deaths, respectively. Both tsunamis transported sandy sediments from beaches and beach ridges, and deposited sand sheets across broad coastal lowland regions (Moore et al., 2006; Naruse et al., 2010; Goto et al., 2011; Shishikura et al., 2012; Takashimizu et al., 2012). Age dating of ancient sandy tsunami deposits is essential for determining the recurrence interval and size of mega-tsunamis over timescales of several thousand years (e.g., Minoura et al., 2001; Monecke et al., 2008; Shishikura et al., 2010; Sawai et al., 2012; Kitamura et al., 2013; Kitamura, 2016). Depositional ages of tsunami deposits are commonly based on ^{14}C dating. However, in case of tsunami events with a recurrence interval of 200 years, such as those occurring in the Nankai trough (Ando, 1975), the Kuril trench (Satake et al., 2005), and south-central Chile (Cisternas et al., 2005), the analytical error of the dated samples (especially marine specimens) are generally too large to identify tsunamis. Using a combination of ^{14}C dating and oxygen-isotope ($\delta^{18}O$) profiles of

articulated bivalves derived from tsunami deposits, it is possible to determine both the absolute age of a tsunami and the season of the year in which it occurred (Kingston, 2016). Articulated bivalves are targeted in such analyses, as they are assumed to have undergone transport and burial alive as a result of a tsunami (Kingston, 2016).

Before the occurrence of the 2011 off the Pacific coast of Tohoku earthquake, the largest tsunami recorded in Japan was the Meiwa tsunami of 24 April AD 1771. The tsunami struck Ishigaki and Miyako Islands along the southern Ryukyu Trench (Fig. 1), and resulted in ~12,000 deaths (Kawana and Nakata, 1994). Based on historical records, the run-up heights of this tsunami were up to 27 m (Kawana and Nakata, 1994; Goto et al., 2010). That event and earlier tsunamis left numerous tsunami boulders in island areas (Kato and Kimura, 1983; Kawana and Nakata, 1994). Examination of tsunami boulders has provided information about the recurrence intervals of large tsunamis, but no information about tsunami size (Goto et al., 2010; Araoka et al., 2013). This is because tsunami run-up heights cannot be reconstructed from the distribution of tsunami boulders, although they can be determined from the landward margins of sandy tsunami deposits (MacInnes et al., 2009; Abe et al., 2012). However, sandy tsunami deposits have not been found on Ishigaki and neighboring islands.

Ando et al. (2018) identified four tsunami deposits (I–IV) in an excavated trench on Ishigaki Island, southwest Japan (Fig. 2). Although there is no terrestrial organic material (e.g., seeds, tree branches, or plant debris) in he tsunami deposits, well-preserved molluscs and corals were collected for radiocarbon dating. ^{14}C dating showed that deposits I–IV were deposited after 248 cal. yr BP, at 920–620 cal. yr BP, at 1670–1250 cal. yr BP, and at 2700–2280 to 1670–1250 cal. yr BP, respectively. Ando et al. (2018) also concluded that deposit I was caused by the AD 1771 Meiwa tsunami.

During the trench survey of Ando et al. (2018), the first author collected well-preserved, articulated marine bivalves, two specimens from deposit I and two from deposit II. The shells were tightly closed and empty inside. The inner and outer shell surfaces did not exhibit encrusting epifauna or evidence of abrasion and dissolution. The ^{14}C ages of the two shells from each tsunami deposit are nearly identical to one another (Fig. 2). Ando et al. (2018) therefore concluded that the shells were transported and buried alive by tsunamis. A similar interpretation was made by Reinhardt et al. (2006) and Donato et al. (2008), who concluded that the presence of allochthonous articulated bivalves in tsunami deposits in Israel or Oman indicates transport of live specimens over a large distance. In these previous studies, the premise is that these articulated shells should would all die at the same time, vs other processes that maybe more gradual (i.e. changes in water conditions).

In Ishigaki Island, Suzuki et al. (2008) identified the emerged massive *Porites* coral boulders using a combination of ^{14}C dating and $\delta^{18}O$ profiles. But, bivalves in tsunami deposits are advantageous, because live transport (articulated specimens) can be recognized versus gastropods, foraminifera and corals (Donato et al., 2008).

In the present study, we analyze the $\delta^{18}O$ profiles of these specimens to reconstruct the seasonal timing of the two tsunamis in Ishigaki Island.

2. Study site

The trench site is located at a farm on Ibaruma, Ishigaki Island (Fig. 1). The elevation of the trench site is approximately 3–10 m above sea level. The reef located off the study area is 1320 m wide and consists of a reef crest, a reef pavement, and a shallow lagoon that is <4.0 m deep (Hongo and Kayanne, 2009). Based on the sea surface temperature (SST) recorded in

Ishigaki Port from 1914 to 2000 (Mishima et al., 2010), the seasonal SST ranges from 19–20°C (February) to 29–30°C (late August to early September). Abe et al. (2009) produced continuous $\delta^{18}O$ records of sea surface water ($\delta^{18}O_{sw}$) for Ishigaki Port from 1998 to 2004. The annual mean value is 0.22 ‰, with a range of −0.1‰ to 0.4‰.

3. Samples and methods

The bivalve specimens analyzed in this study are *Fragum loochooanum* and *F. unedo* for deposit I and *Regozara flavum* and *Mactra maculata* for deposit II. As the thickness of the outer shell layer of *F. unedo* was too thin to collect powdered carbonate samples, we did not perform an $\delta^{18}O$ analysis on this specimen. Both *F. loochooanum* and *R. flavum* inhabit sandy substrata in the lower intertidal zone to a depth of 20 m (Okutani, 2000). *M. maculata* lives in the lower intertidal zone to a depth of 30 m (Okutani, 2000).

The specimens were embedded directly in polyester resin without any chemical treatment, and cut along the axis of maximum growth. The sections were ground with 1200 SiC grit. Powdered carbonate samples were collected from the outer shell layer using an automated Micromill sampler at the Japan Agency for Marine-Earth Science and Technology (JAMSTEC), Yokosuka, Japan (Sakai and Kodan, 2011). Individual milling steps ranged between ca. 550 and 1000 μm perpendicular to the direction of growth. Each milling yielded 40–120 mg of aragonite powder. The powdered carbonate samples received no additional thermal or chemical treatment prior to $\delta^{18}O$ analysis. The sample was analyzed using a mass spectrometer (IsoPrime, Micromass) at JAMSTEC. Individual samples were reacted with 100% phosphoric acid at 90°C. Oxygen and carbon isotope values of shell carbonate ($\delta^{18}O_{shell}$ and $\delta^{13}C_{shell}$) are reported relative to the Peedee Belemnite (PDB), and the analytical

117 precision (1σ) was better than ±0.1‰ in all cases. X-ray diffractometer analysis revealed that
118 the shells consist entirely of aragonite.
119 No previous study has investigated the lifespans of *F. loochooanum*, *R. flavum* and *M.*
120 *maculate*, however, the lifespans of closely related species are 5 years (*Fragum fragum*), 5
121 years (*Acrosterigma burchardi*), and 12 years (*Mactra chinensis*), (Limpanont et al., 2010;
122 Moss et al., 2016). Thus, the lifespans of the study species may reach 5 years.
123
124 **4. Results**
125 The $\delta^{18}O_{shell}$ values of *F. loochooanum* from deposit I are between −0.23‰ and −1.46‰,
126 and become heavier and then lighter toward the distal end (Fig. 3). Except for one
127 exceptionally light $\delta^{18}O$ value (−4.73‰), $\delta^{18}O_{shell}$ of *R. flavum* from deposit II ranges from
128 −3.04‰ to −1.79‰, and exhibits two cycles of becoming lighter and then heavier toward the
129 shell margin (Fig. 3). The $\delta^{18}O_{shell}$ values of *M. maculata* from deposit II are −2.70‰ to
130 −1.21‰, becoming lighter and then heavier toward the distal region (Fig. 3).
131
132 **5. Discussion**
133 It is widely accepted that biogenic aragonite is precipitated at or very near $\delta^{18}O$
134 equilibrium with the ambient water, and that deviations from the $\delta^{18}O$ equilibrium can be
135 accounted for by species-specific vital effects operating during the precipitation of the
136 biogenic aragonite (Kim et al., 2007). To accurately reconstruct the water temperature from
137 the $\delta^{18}O$ compositions of *F. loochooanum*, *R. flavum*, and *M. maculata*, temperature
138 equations ($\delta^{18}O_{shell}$-derived temperatures) for each studied species must be used. As equations
139 have not been published for the species used in the present study, we applied $\delta^{18}O_{shell}$-derived

140 temperatures using six published temperature equations for abiogenic and biogenetic
141 aragonite (Dunbar and Wefer, 1984; Grossman and Ku, 1986; Patterson et al., 1993; Carré et
142 al., 2005; Kim et al., 2007; Aubert et al., 2009; Fig. 3). Based on data presented by Abe et al.
143 (2009), we used a $\delta^{18}O_{sw}$ value of 0.22‰ for the study area.

144 For the most part, the $\delta^{18}O_{shell}$-derived temperatures based on five previously published
145 equations fall within the same temperature range (Fig. 3). However, in the cases of *R. flavum*
146 and *M. maculata*, most values obtained using the equation of Grossman and Ku (1986) are
147 higher than the maximum SST. Thus, we excluded this equation in our discussion, along with
148 the exceptionally light $\delta^{18}O$ value (−4.73‰) of *R. flavum*.

149 The $\delta^{18}O_{shell}$-derived temperatures of *F. loochooanum* in tsunami deposit I decreased and
150 then increased toward the margin of the shell (Fig. 3). The range (3.5–5.9°C) corresponds to
151 35%–59% of a temperature range of 10°C. In the case of the minimum $\delta^{18}O_{shell}$-derived
152 temperature, except for the value (17.1°C) obtained using the equation of Kim et al. (2007),
153 the results are equal to (19.1–20.7°C) or slightly higher than (22.7°C) the minimum monthly
154 SST (19–20°C). In contrast, the highest $\delta^{18}O_{shell}$-derived temperature (23.0–26.2°C) is
155 inferred to be at the shell margin, corresponding to the spring SST. Thus, we deduce that the
156 $\delta^{18}O_{shell}$-derived temperatures of *F. loochooanum* correspond to the change from fall of the
157 previous year to spring, and that the time of death was spring. This result confirms that
158 deposit I was related to the Meiwa tsunami of 24 April AD 1771, and provides information of
159 region specific reservoir age (ΔR).

160 Ando et al. (2018) estimated ^{14}C ages of *F. loochooanum* and *F. unedo* using $\Delta R = -36 \pm$
161 78. The value was determined from coral of Ishigaki Island for AD 1947–1950 by Hirabayahi
162 et al. (2017). Given that the calendar ages of the two shells are AD 1771, ΔR of samples are

calculated as −38 ± 19 and −111 ± 29 years, respectively. Hirabayahi et al. (2017) reported that seasonal-scale fluctuations of ΔR at AD 1947–1950 range from −136 ± 42 to 62 ± 50. Thus, we think that the difference in ΔR of two shells may be explained by difference of periods of the ^{14}C dated portion and seasonal-scale fluctuations of ΔR.

The $\delta^{18}O_{shell}$-derived temperatures of *R. flavum* in tsunami deposit II show two cycles. The maximum $\delta^{18}O_{shell}$-derived temperatures are equal to (29.3–30.7°C) or slightly higher than (31.1–31.8°C) the maximum monthly SST (29–30°C), while the minimum $\delta^{18}O_{shell}$-derived temperature (24.6–27.2°C) is 4–7°C higher than the minimum monthly SST (19–20°C). This discrepancy in the minimum temperatures implies a slowdown or cessation of shell growth between fall and spring. We therefore propose that the shell portion of *R. flavum* formed over a period of 2 years, and that the time of death was fall because the last $\delta^{18}O_{shell}$-derived temperature is slightly lower than the midpoint of the maximum and minimum $\delta^{18}O_{shell}$-derived temperatures.

The $\delta^{18}O_{shell}$-derived temperatures of *M. maculata* in tsunami deposit II increased and then decreased toward the margin of the shell (Fig. 3). The maximum $\delta^{18}O_{shell}$-derived temperatures are equal to (29.2–30.3°C) or slightly lower than (28.1°C) the maximum monthly SST (29–30°C). The minimum $\delta^{18}O_{shell}$-derived temperature (21.8–25.5°C) was obtained from the sample at the shell margin, and is 2–6°C higher than the minimum monthly SST (19–20°C). We conclude that the shell portion of *M. maculata* formed from spring of the previous year to fall, and that the animal died during fall. The difference in $\delta^{18}O_{shell}$-derived temperature between *R. flavum* and *M. maculate* in tsunami deposit II is explained by difference of species-specific vital effects and/or different habitats.

In summary, the $\delta^{18}O_{shell}$ profiles of *R. flavum* and *M. maculata* indicate that tsunami deposit II was caused by a tsunami in the fall of a year during the period 920–620 cal. yr BP. From the historical document Miyakojima-Kyuki ("Old Records of Miyako Island"), which was written at about AD 1748 and did not mention the years in which events occurred, Shimoji (2007) inferred that large tsunamis struck the Miyako Island around the 14th century and in the late 15th century. Our results cannot be used to assess the validity of this interpretation of historical documents, although they provide important information for studies of tsunamis in the south Ryukyu islands during the 14th and15th centuries.

6. Conclusions

This study analyzed the $\delta^{18}O$ profiles of two well-preserved and articulated marine bivalves from each of sandy tsunami deposits I and II on Ishigaki Island along the southern Ryukyu Trench. Our results show that shell death in deposits I and II occurred during spring and fall, respectively. The season of shell death in tsunami deposit I supports that the deposit was generated by the 1771 Meiwa tsunami, which therefore provides a region-specific radiocarbon reservoir age. The season of shell death in tsunami deposit II provides a constraint on the tsunami that formed the deposit. A combination of taphonomic study, radiometric dating, and analysis of the $\delta^{18}O$ profiles of bivalve shells derived from tsunami deposits provides important chronologic constraints on the tsunami events that formed the deposits.

Acknowledgements

We acknowledge constructive reviews from anonymous reviewers and suggestions by the Editor, Prof. Shu Gao, for improvements. We thank Dr. Masataka Ando and Toshiyuki Chinen for our survey on Ishigaki Island. This study was supported by Grants-in-Aid (17H02972) awarded by the Japan Society for the Promotion of Science and the Integrated Center for Education and Research of Natural Hazards, Shizuoka University.

References

Abe, O., Agata, S., Morimoto, M., Abe, M., Yoshimura, K., Hiyama, T., Yoshida, N., 2009. A 6.5 year continuous record of sea surface salinity and seawater isotopic composition at Harbour of Ishigaki Island, southwest Japan. Isotopes Environ. Health Stud. 45, 1–12.

Abe, T., Goto, K., and, Sugawara, D., 2012. Relationship between the maximum extent of tsunami sand and the inundation limit of the 2011 Tohoku-oki tsunami on the Sendai Plain, Japan. Sediment. Geol. 282, 142–150.

Ando, M., 1975. Source mechanisms and tectonic significance of historical earthquakes along the Nankai trough, Japan. Tectonophysics. 27, 119–140.

Ando, M., Kitamura, A., Tu, Y., Ohashi, Y., Imai, T., Nakamura, M., Ikuta, R., Miyari, Y., Yokoyama, Y., Shishikura, M., 2018. Source of high tsunamis along the southernmost Ryukyu trench inferred from tsunami stratigraphy. Tectonophysics. 722, 265–276.

Araoka, D., Yokoyama, Y., Suzuki, A., Goto, K., Miyagi, K., Miyazawa, K., Matsuzaki, H., Kawahata, H., 2013. Tsunami recurrence revealed by Porites coral boulders in the southern Ryukyu Islands, Japan. Geology. 41, 919–922.

Aubert, A., Lazareth, C., Cabioch, G., Boucher, H., Yamada, T., Iryu, Y., Farman, R., 2009. The tropical giant clam *Hippopus hippopus* shell, a new archive of environmental conditions as revealed by sclerochronological and $\delta^{18}O$ profiles. Coral Reefs. 28, 989–998.

Carré, M., Bentaleb, I., Blamart, D., Ogle, N., Cardenas, F., Zevallos, S., Kalin, R.M., Ortlieb, L., Fontugne, M., 2005. Stable isotopes and sclerochronology of the bivalve *Mesodesma donacium*: potential application to Peruvian paleoceanographic reconstructions. Palaeogeogr Palaeoclimatol Palaeoecol. 228, 4-25.

Cisternas, M., et al. 2005. Predecessors of the giant 1960 Chile earthquake. Nature. 437, 404–407.

Donato, S.V., Reinhardt, E.G., Boyce, J.I., Rothaus, R., Vosmer, T., 2008. Identifying tsunami deposits using bivalve shell taphonomy. Geology. 36, 199-202.

Dunbar, R.B., Wefer, G., 1984. Stable isotope fractionation in benthic foraminifera from Peruvian continental margin. Mar. Geol. 59, 215–225.

Goto, K., Kawana, T., Imamura, F., 2010. Historical and geological evidence of boulders deposited by tsunamis, southern Ryukyu Islands, Japan. Earth-Sci. Rev. 102, 77–99.

Grossman, E., Ku, T., 1986. Oxygen and carbon isotope fractionation in biogenic aragonite: temperature effects. Chem. Geol. 59, 59–74.

Hirabayashi, S., Yokoyama, Y., Suzuki, A., Miyairi, Y., Aze, T., 2017. Short-term fluctuations in regional radiocarbon reservoir age recorded in coral skeletons from the Ryukyu Islands in the north-western Pacific. J. Quat. Sci. 32, 1–6.

Hongo, C., Kayanne, H., 2009. Holocene coral reef development under windward and leeward locations at Ishigaki Island, Ryukyu Islands, Japan. Sediment. Geol. 214, 62–73.

Kato, Y., Kimura, M., 1983. Age and origin of so-called “Tsunami-ishi”, Ishigaki Island, Okinawa prefecture. J. Geol. Soc. Japan. 89, 471–474 (in Japanese with English abstract).

Kawana, T., Nakata, T., 1994. Timing of Late Holocene tsunamis originated around the southern Ryukyu Islands, Japan, deduced from coralline tsunami deposits. J. Geogra. Japan. 103, 352-376, (in Japanese with English abstract).

Kim, S.-T., O’Neil, J.R., Hillaire-Marcel, C., Mucci, A., 2007. Oxygen isotope fractionation between synthetic aragonite and water: Influence of temperature and Mg^{2+} concentration. Geochim. Cosmochim. Acta. 71, 4704–4715.

Kingston, A., 2016. High-resolution stable isotope analysis of biogenic carbonates as proxy evidence for Holocene environmental change: examples from authigenic lake carbonate and bivalve isotope profiles [Ph.D. thesis]: Saskatoon, University of Saskatchewan, 221 p. https://ecommons.usask.ca/handle/10388/7652 (November 2017).

Kitamura, A., 2016. Examination of the largest-possible tsunamis (Level 2 tsunami) generated along the Nankai and Suruga troughs during the past 4000 years based on studies of tsunami deposits from the 2011 Tohoku-oki tsunami. Prog. Earth Planet. Sci. 3:12 https://doi.org/10.1186/s40645-016-0092-7

Kitamura, A., Fujiwara, O., Shinohara, K., Akaike, S., Masuda, T., Ogura, K., Urano, Y., Kobayashi, K., Tamaki, C., Mori, H., 2013. Identifying possible tsunami deposits on the Shizuoka Plain, Japan and their correlation with earthquake activity over the past 4000 years. The Holocene. 23, 1682–1696.

Limpanont, Y., Yang, H.-Y., Won,,S.-H., Han, S.-J., Lee, J.-B., Lee, B.-G., Choi, K.-S., 2010. First report on the annual reproductive cycle of Burchardi’s cockle, *Acrosterigma*

(=*Vasticardium*) *burchardi* Dunker 1877 (Bivalvia: Cardiidae) on a subtidal sand flat off southern Jeju Island, Korea. Invertebr Repr Dev. 54, 27–34.

MacInnes, B.T., Bourgeois, J., Pinegina, T.K., Kravchunovskaya, E.A., 2009. Tsunami geomorphology: Erosion and deposition from the 15 November 2006 Kuril Island tsunami. Geology. 37, 995–998.

Minoura, K., Imamura, F., Sugawara, D., Kono, Y., Iwashita, T., 2001. The 869 Jogan tsunami deposit and recurrence interval of large-scale tsunami on the Pacific coast of northeast Japan. J. Nat. Disaster Sci. 23, 83–88.

Mishima, M., Suzuki, A., Nagao M., Ishimura, T., Inoue, M., and Kawahata, H., 2010. Abrupt shift toward cooler condition in the earliest 20th century detected in a 165 year coral record from Ishigaki Island, southwestern Japan. Geophys. Res. Lett. 37, L15609, doi:10.1029/2010GL043451

Monecke, K,. Finger, W., Klarer, D., Kongko, W., McAdoo, B.G., Moore, A.L., Sudrajat, S.U., 2008. A 1,000-year sediment record of tsunami recurrence in northern Sumatra. Nature. 455, 1232–1234.

Moore, A.L., Nishimura, Y., Gelfenbaum, G., Kamataki, T., Triv, R., 2006. Sedimentary deposits of the 26 December 2004 tsunami on the northwest coast of Aceh, Indonesia: Earth, Planets Space. 58, 253−258.

Moss, D.K., Ivany, L.C., Judd, E.J., Cummings, P.W., Bearden, C.E., Kim, W-J., Artruc, E.G., Driscoll, J.R., 2016. Lifespan, growth rate, and body size across latitude in marine Bivalvia, with implications for Phanerozoic evolution. Proc R Soc B 283(1836):20161364. doi: 10.1098/rspb.2016.1364

294 Naruse, H., Fujino, S., Suphawajruksakul, A., Jarupongsakul, T., 2010. Features and formation
295 processes of multiple deposition layers from the 2004 Indian Ocean Tsunami at Ban Nam
296 Kem, southern Thailand. Island Arc. 19, 399–411.
297 Okutani, T., 2000. Marine Mollusks in Japan. University of Tokyo Press, 1173 pp.
298 Patterson, W.P., Smith, G.R., Lohmann, K.C. 1993. Continental paleothermometry and
299 seasonality using the isotopic composition of aragonitic otoliths of freshwater fishes.
300 Geophys. Monograph. 78, 191–202.
301 Reinhardt, E.G., Goodman, B.E., Boyce, J.I., Lopez, G., van Hengstum, P., Rink, W., Mart, Y.,
302 Raban, A. 2006. The tsunami of December 13, 115 A.D. and the destruction of Herod the
303 Great's harbor at Caesarea Maritima, Israel. Geology. 34, 1061–1064.
304 Sakai, S., and Kodan, T., 2011. Micropowder collecting technique for stable isotope analysis of
305 carbonates. Rapid Commun. Mass Spectrom. 25, 1205–1208.
306 Satake, K., Nanayama, F., Yamaki, S., Tanioka, Y., Hirata, K., 2005. Variability among tsunami
307 sources in the 17th-21st centuries along the southern Kuril trench, *in* Satake, K. ed, In
308 Tsunamis: Case Studies and Recent Developments. Dordrecht, Springer, 157–170.
309 Sawai, Y., Namegaya, Y., Okamura, Y., Satake, K., Shishikura, M., 2012. Challenges of
310 anticipating the 2011 Tohoku earthquake and tsunami using coastal geology. Geophys. Res.
311 Lett. 39, L21309, doi:10.1029/2012GL053692.
312 Shimoji, K., 2007. Regional history of Amare village and ancient tsunamis in Miyako Island,
313 Okinawa, Japan. Bull. Miyakojima City Mus. 11, 1−12 (in Japanese)
314 Shishikura, M., Sawai, Y., Namegaya, Y., 2010. Reproduction of mega-tsunami that occurred in
315 Heian period AD 869 Jogan tsunami. AFREC News, 16, 1−10 (in Japanese)

316 Shishikura, M., Fujiwara, O., Sawai, Y., Namegaya, Y., Tanigawa, K., 2012. Inland-limit of the
317 tsunami deposit associated with the 2011 off-Tohoku earthquake in the Sendai and
318 Ishinomaki Plains, Northeastern Japan. Ann. Rep. Active Fault and Paleoearthquake Res. 12,
319 45–61 (in Japanese with English abstract)
320 Suzuki, A., Yokoyama, Y., Kan, H., Minoshima, K., Matsuzaki, H., Hamanaka, N., Kawahata,
321 H., 2008. Identification of 1771 Meiwa Tsunami deposits using a combination of
322 radiocarbon dating and oxygen isotope microprofiling of emerged massive *Porites* boulders.
323 Quat Geochronol. 3, 226–234.
324 Takashimizu, Y., Urabe, A., Suzuki, K., Sato, Y., 2012. Deposition by the 2011 Tohoku-oki
325 tsunami on coastal lowland controlled by beach ridges near Sendai, Japan. Sediment. Geol.
326 282, 124–141.
327

328 Figure captions

329 Fig. 1. (a) Plate boundaries around the southern Ryukyu Islands (after Ando et al., 2009). EU:
330 Eurasia Plate; NA: North American Plate; PC: Pacific Plate; PS: Philippine Sea Plate; MY:
331 Miyako Island. 1: epicenter of the 2011 Tohoku-oki earthquake (Mw 9.0). (b) Ishigaki Island,
332 showing the location of the study area and the tsunami run-up heights (m) in 1771 on Ishigaki
333 island (after Goto et al., 2010). (c) Photograph of the study trench.

334

335 Fig. 2 (a) Columnar sections of the study trench, modified from Ando et al. (2018). (b) ^{14}C
336 age probability distributions (cal. yr BP) showing 95% error bars for studied shell samples
337 (Ando et al., 2018). The ages were translated into a calendar timescale using the program
338 OxCal4.1 (Brank Ramsey, 2009), based on comparisons with the IntCal13 data (Reimer et al.,
339 2013), after applying a local marine correction for the Ishigaki area of $\Delta R = -36 \pm 78$
340 (Hirabayahi et al., 2017). (c) Mode of occurrence of *Regozara flavum.*

341

342 Fig. 3 Records (left panel) of $\delta^{18}O_{shell}$ and $\delta^{13}C_{shell}$ versus distance from the ventral margin of
343 the shell. Note that the $\delta^{18}O_{shell}$ axis has been inverted. Reconstructed temperature record
344 (right panel) based on $\delta^{18}O_{shell}$. *Fragum loochooanum* (upper panel) was collected from
345 tsunami deposit I. *Regozara flavum* and *Mactra maculate* (middle and lower panels) were
346 collected from tsunami deposit II.

347

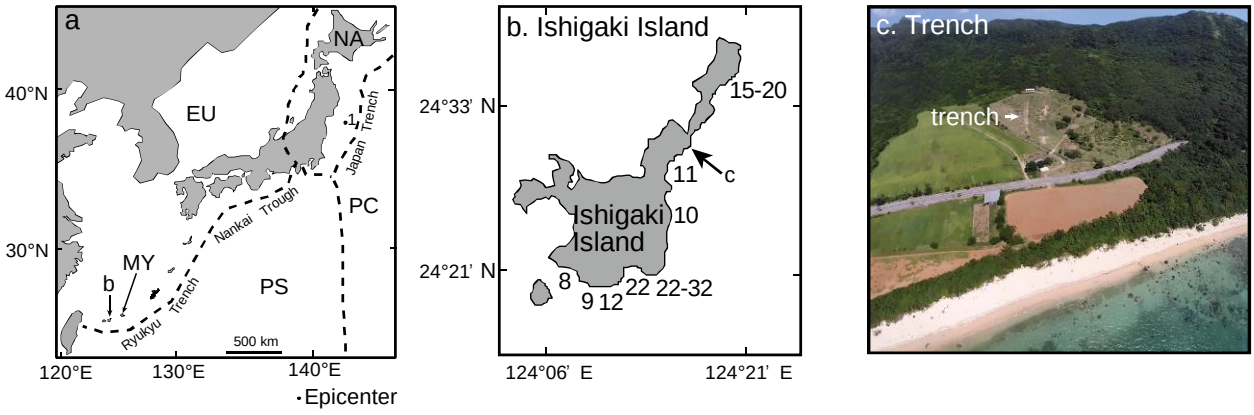

348

Fig. 1

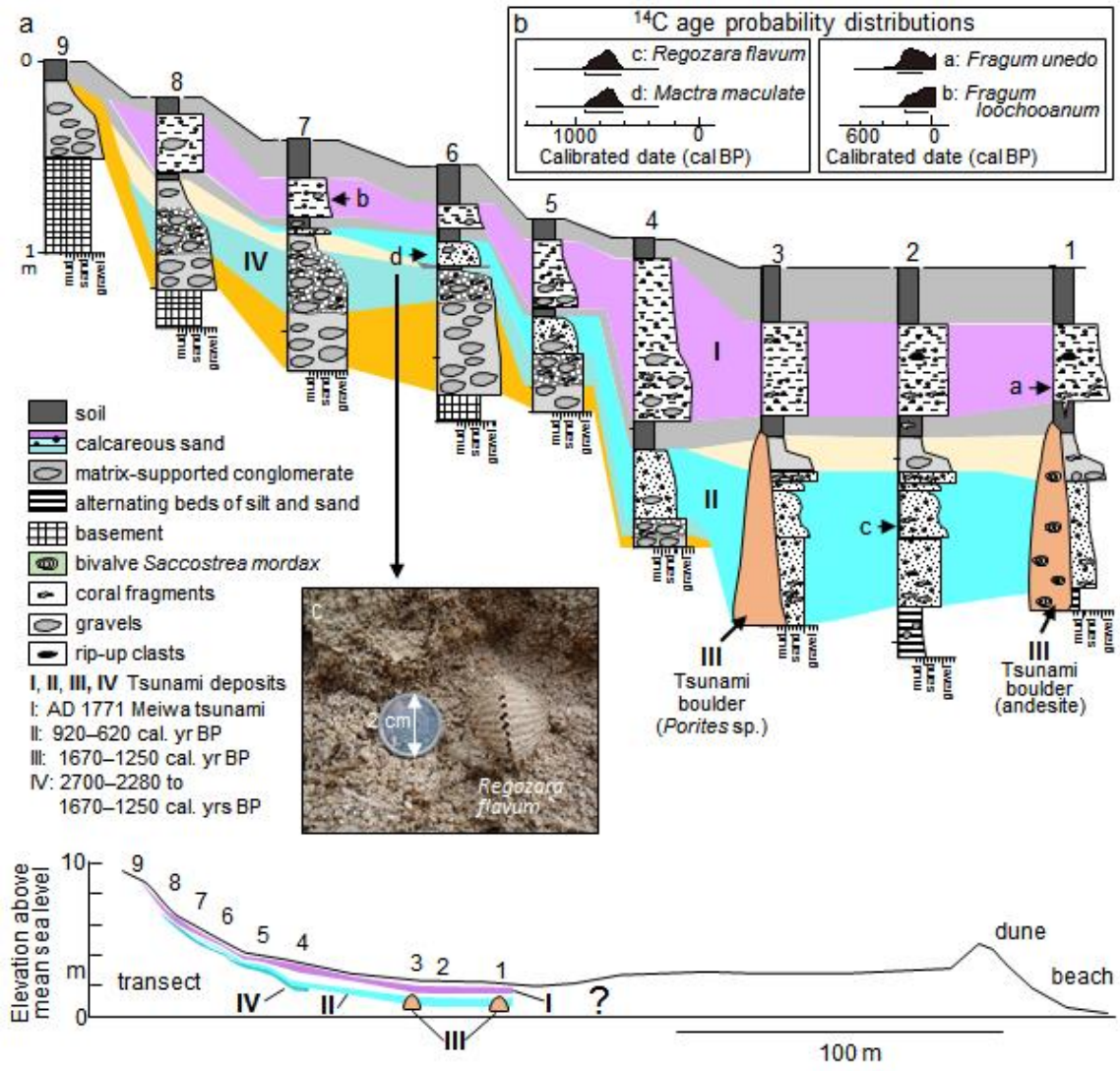

Fig. 2

349

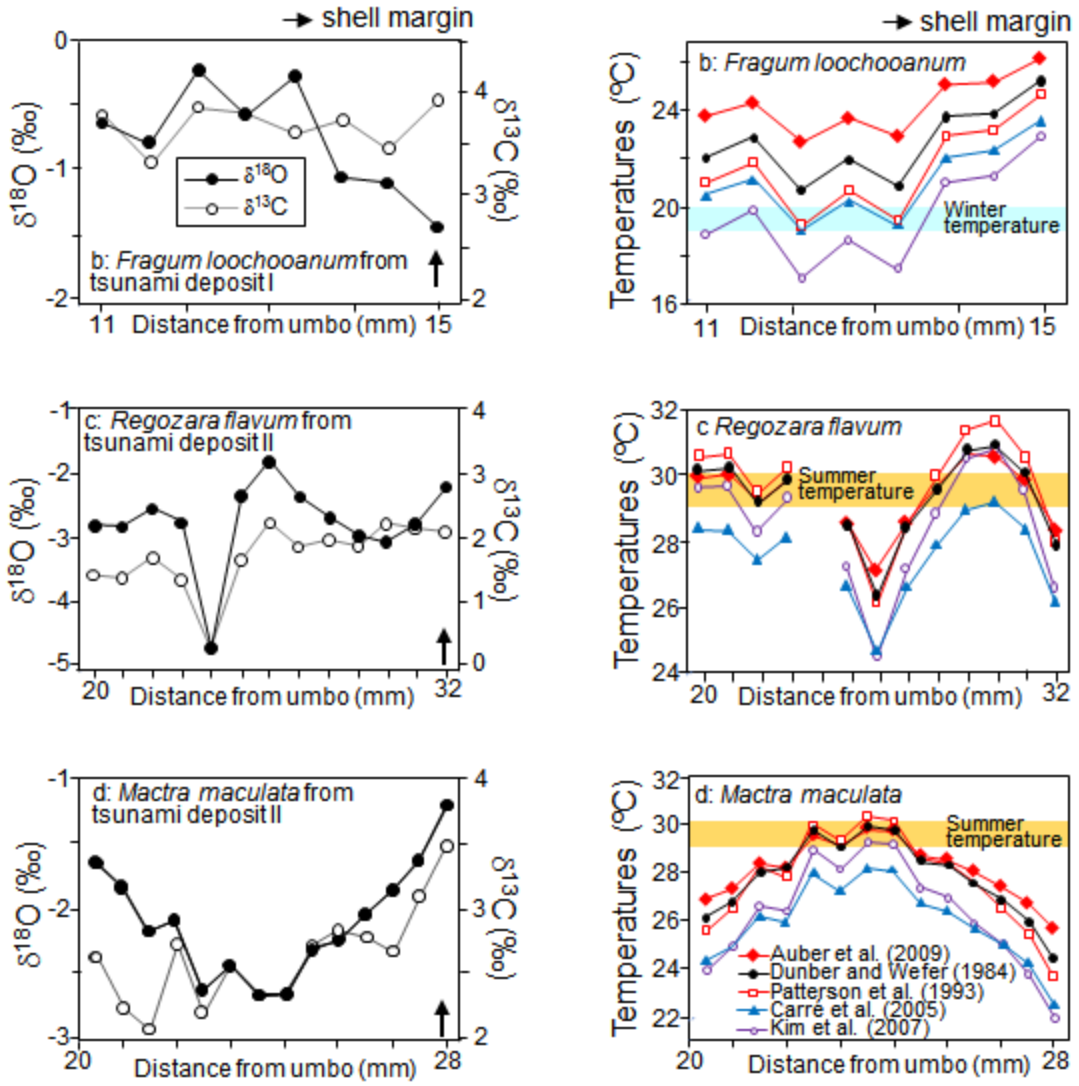
shell margin
δ18O (‰)
δ13C (‰)
δ18O
δ13C
b: Fragum loochooanum from tsunami deposit I
11 Distance from umbo (mm) 15
shell margin
Temperatures (ºC)
b: Fragum loochooanum
Winter temperature
11 Distance from umbo (mm) 15
c: Regozara flavum from tsunami deposit II
20 Distance from umbo (mm) 32
c Regozara flavum
Summer temperature
20 Distance from umbo (mm) 32
d: Mactra maculata from tsunami deposit II
20 Distance from umbo (mm) 28
d: Mactra maculata
Summer temperature
Auber et al. (2009)
Dunber and Wefer (1984)
Patterson et al. (1993)
Carré et al. (2005)
Kim et al. (2007)
20 Distance from umbo (mm) 28

Fig. 3

350

351